Chinese Physics B

RAPID COMMUNICATION

Discontinuous and continuous transitions of collective behaviors in living systems*

To cite this article: Xu Li *et al* 2021 *Chinese Phys. B* **30** 128703

Chin. Phys. B Vol. 30, No. 12 (2021) 128703

RAPID COMMUNICATION

Discontinuous and continuous transitions of collective behaviors in living systems*

Xu Li(李旭)[1,2,†], Tingting Xue(薛婷婷)[1,†], Yu Sun(孙宇)[2], Jingfang Fan(樊京芳)[1,2], Hui Li(李辉)[1,2], Maoxin Liu(刘卯鑫)[3], Zhangang Han(韩战钢)[1], Zengru Di(狄增如)[1,2], and Xiaosong Chen(陈晓松)[1,2,‡]

[1] School of Systems Science, Beijing Normal University, Beijing 100878, China
[2] Institute of Nonequilibrium Systems, Beijing Normal University, Beijing 100878, China
[3] School of Science, Beijing University of Posts and Telecommunications, Beijing 100876, China

(Received 16 November 2021; revised manuscript received 22 November 2021; accepted manuscript online 23 November 2021)

Living systems are full of astonishing diversity and complexity of life. Despite differences in the length scales and cognitive abilities of these systems, collective motion of large groups of individuals can emerge. It is of great importance to seek for the fundamental principles of collective motion, such as phase transitions and their natures. Via an eigen microstate approach, we have found a discontinuous transition of density and a continuous transition of velocity in the Vicsek models of collective motion, which are identified by the finite-size scaling form of order-parameter. At strong noise, living systems behave like gas. With the decrease of noise, the interactions between the particles of a living system become stronger and make them come closer. The living system experiences then a discontinuous gas–liquid like transition of density. The even stronger interactions at smaller noise make the velocity directions of the particles become ordered and there is a continuous phase transition of collective motion in addition.

Keywords: living systems, phase emergence, phase transitions, eigen mircostate

PACS: 87.10.–e, 05.70.Fh, 64.60.Ht, 89.75.−k **DOI:** 10.1088/1674-1056/ac3c3f

1. Introduction

Collective behaviors are the most important properties of systems consisting of many individuals. Collective motion of large groups of individuals is a truly fascinating collective behavior in living systems and was observed in starlings,[1–3] bacterial communities,[4,5] ant colonies,[6,7] locusts,[8] midges,[9,10] sheep,[11] etc. While detailed case studies are preferred in general by biologists,[8,12,13] physicists usually seek for universal features behind seemingly diverse observations and the models sufficient to capture the fundamental features[14] to find the fundamental principles of collective motion.

It is the mission of statistical physics to connect the microscopic properties of individual with the macroscopic behavior using the probability theory and statistics.[15–17] In addition, the studies of phase transitions and critical phenomena[18] need to identify order-parameters in advance.

As a prototype model of collective motion in living systems, the standard Viscek model (SVM)[19] was introduced. In the original work of SVM, it was claimed that phase transition of collective motion is continuous. But this was challenged later by Chaté *et al.*[20,21] They showed that the continuous nature observed is actually due to finite-size effects and the phase transition is discontinuous. Since the precise order-parameter of collective motion is unknown and no systematic analysis of finite-size scaling has been made, these results about the nature of phase transitions until now are not conclusive.

In an eigen microstate approach developed recently,[22,23] collective behaviors of systems are indicated by the condensation of eigen microstate in statistical ensemble,[24] which is analogous to the Bose–Einstein condensation of Bose gases.[25] The approach has been applied successfully to study the phase transitions of Ising models.[22,23] Here we use this approach to investigate collective behaviors of living systems and identify order-parameters and the nature of phase transitions precisely.

2. Eigen microstates and phase transitions

2.1. Microstates

For a particle i of a living system, its state is characterized by velocity $\boldsymbol{v}_i(t)$ and position $\boldsymbol{x}_i(t)$. It is more relevant to introduce neighborhood density of i as $n_i(t) = N_i(t)/(2r)^2$, where r is the interaction distance and $N_i(t)$ is the number of the particles around i within a square with side length $2r$. From states of N components at $t = 1,2,\ldots,M$, we can obtain the average velocity and neighborhood density as

$$\bar{v} = \sqrt{\frac{1}{MN}\sum_{t=1}^{M}\sum_{i=1}^{N}|\boldsymbol{v}_i(t)|^2}, \tag{1}$$

$$\bar{n} = \frac{1}{MN}\sum_{t=1}^{M}\sum_{i=1}^{N}n_i(t). \tag{2}$$

*Project supported by the Fundamental Research Funds for the Central Universities, China (Grant No. 2019XD-A10) and the National Natural Science Foundation of China (Grant No. 71731002).

†These authors contributed equally.

‡Corresponding author. E-mail: chenxs@bnu.edu.cn

We describe the state of particle i with $\bar{v}_{i,x}(t) = v_{i,x}(t)/\bar{v}$, $\bar{v}_{i,y}(t) = v_{i,y}(t)/\bar{v}$, and $\delta n_i(t) = (n_i(t) - \bar{n})/\bar{n}$. Using the states of N components, we can define the microstate of the living system as

$$\boldsymbol{S}(t) = \begin{bmatrix} \boldsymbol{s}_1(t) \\ \boldsymbol{s}_2(t) \\ \vdots \\ \boldsymbol{s}_N(t) \end{bmatrix}, \tag{3}$$

where

$$\mathbf{s}_i(t) = \begin{bmatrix} \bar{v}_{i,x}(t) \\ \bar{v}_{i,y}(t) \\ \delta n_i(t) \end{bmatrix}. \tag{4}$$

2.2. Eigen microstates[22]

Using M microstates of the living system, a statistical ensemble[24] can be composed and characterized by an $N_{\mathrm{T}} \times M$ matrix $\boldsymbol{A}$ with $N_{\mathrm{T}} = 3N$ and elements[22]

$$A_{it} = s_i(t)/\sqrt{C_0}, \tag{5}$$

where $C_0 = \sum_{t=1}^{M} \sum_{i=1}^{N_{\mathrm{T}}} s_i^2(t)$.

The correlations between microstates and states of particles[26] can be presented respectively by an $M \times M$ matrix and an $N_{\mathrm{T}} \times N_{\mathrm{T}}$ matrix as

$$\boldsymbol{C} = \boldsymbol{A}^{\mathrm{T}} \cdot \boldsymbol{A}, \tag{6}$$

$$\boldsymbol{K} = \boldsymbol{A} \cdot \boldsymbol{A}^{\mathrm{T}}. \tag{7}$$

Using eigenvectors of $\boldsymbol{C}$ and $\boldsymbol{K}$, we can compose two unitary matrices

$$\boldsymbol{V} = [\boldsymbol{v}_1 \boldsymbol{v}_2 \ldots \boldsymbol{v}_M], \quad \boldsymbol{U} = [\boldsymbol{u}_1 \boldsymbol{u}_2 \ldots \boldsymbol{u}_{N_{\mathrm{T}}}]. \tag{8}$$

According to the singular value decomposition (SVD),[27] the ensemble matrix $\boldsymbol{A}$ can be factorized as

$$\boldsymbol{A} = \boldsymbol{U} \cdot \Sigma \cdot \boldsymbol{V}^{\mathrm{T}}, \tag{9}$$

where Σ is an $N_{\mathrm{T}} \times M$ diagonal matrix with elements

$$\Sigma_{IJ} = \begin{cases} \sigma_I, & I = J \le r, \\ 0, & \text{otherwise}, \end{cases} \tag{10}$$

where $r = \min(M, N_{\mathrm{T}})$.

We can rewrite the ensemble matrix $\boldsymbol{A}$ as

$$\boldsymbol{A} = \sum_{I=1}^{r} \sigma_I \boldsymbol{u}_I \otimes \boldsymbol{v}_I, \tag{11}$$

where $\sum_{I=1}^{r} \sigma_I^2 = 1$. σ_I is the probability amplitude. $W_I^{\mathrm{E}} = \sigma_I^2$ is the probability of the eigen microstate $\boldsymbol{u}_I$, whose evolution is described by $\boldsymbol{v}_I$. For disorder living systems, no eigen microstate is dominant so that all probability amplitudes are of the same order. At the limits $M \to \infty$ and $N \to \infty$, all probability amplitudes $\sigma_I \to 0$.

2.3. Phase emergence

If a probability amplitude $\sigma_I \to$ no-zero at the limits $M \to \infty$ and $N \to \infty$, there is a condensation of the eigen microstate $\boldsymbol{u}_I$ in the statistical ensemble. This condensation of eigen microstate is analogous to the Bose–Einstein condensation of Bose gases,[25] in which a finite part of total bosons simultaneously occupy the ground state. This condensation of eigen microstate implies an emergent phase described by $\boldsymbol{u}_I$. More than one emergent phase can exist in a system.

2.4. Phase transition and finite-size scaling

With changes of external conditions or internal conditions of living systems, a probability amplitude σ_I may increase from zero to finite. Now there is a phase transition with order-parameter described by σ_I and new phase characterized by $\boldsymbol{u}_I$.

With external conditions characterized by a parameter η, we have $\eta = \eta_{\mathrm{c}}$ at the phase transition point. The distance from the phase transition point is $h = (\eta - \eta_{\mathrm{c}})/\eta_{\mathrm{c}}$. In the asymptotic region with $|h| \ll 1$, we proposed a finite-size scaling form of σ_I as[22]

$$\sigma_I(\eta, L) = L^{-\beta/\nu} f_I(hL^{1/\nu}), \tag{12}$$

where L is the system size, β is the critical exponent of order parameter, and ν is the critical exponent of correlation length.

For $\beta > 0$, we have $\sigma_I(\eta, \infty) = 0$ at $\eta > \eta_{\mathrm{c}}$ and $\sigma_I(\eta, \infty) \propto (\eta_{\mathrm{c}} - \eta)^{\beta}$ for $\eta < \eta_{\mathrm{c}}$. This is a continuous phase transition.

When $\beta = 0$, there is a jump from $\sigma_I(\eta, \infty) = 0$ at $\eta > \eta_{\mathrm{c}}$ to $\sigma_I(\eta_{\mathrm{c}}, L) = f_I(0) \neq 0$ at η_{c}. This indicates a discontinuous phase transition.

2.5. Global indexes of eigen microstate

To get an overview of $\boldsymbol{u}_I$, we define the collective motion index as

$$\Phi^I = \sqrt{\left| \frac{1}{\sqrt{N}} \sum_{i=1}^{N} v_{i,x}^I \right|^2 + \left| \frac{1}{\sqrt{N}} \sum_{i=1}^{N} v_{i,y}^I \right|^2}, \tag{13}$$

where $(v_{i,x}^I, v_{i,y}^I)$ are the velocity components. The density fluctuation index of $\boldsymbol{u}_I$ is defined as

$$\delta n^I = \frac{1}{\sqrt{N}} \sum_{i=1}^{N} \delta n_i^I, \tag{14}$$

where δn_i^I are the density fluctuation components.

2.6. Spatial distribution of eigen microstate

For an eigen microstate $\boldsymbol{u}_I$, states of all particles are given. We display the state of a particle i at the corresponding average position $\boldsymbol{R}_i = \frac{1}{M} \sum_{t=1}^{M} \boldsymbol{r}_i(t)$. We will show the spatial distributions of velocity and neighborhood density fluctuation separately.

We have applied the eigen microstate approach (EMA) to study successfully the ferromagnetic phase transitions of Ising models in equilibrium.[22] Here the EMA is used to investigate the emergent phases and their phase transitions of nonequilibrium living systems.

3. Results and discussion

3.1. SVM[19]

In a two-dimensional SVM, there are $N = L \times L$ pointwise particles labeled as $1, 2, \ldots, N$ and placed randomly on a two-dimensional domain with size L and periodic boundary conditions. They move synchronously at discrete time steps by a fixed distance $v_0 \Delta t$, where v_0 is the velocity defined as the length of displacement per time step $\Delta t = 1$. Each particle i is endowed with an angle θ_i that determines the direction of the movement during the next time step, and its update is determined by the orientations of its neighbors (defined as particles within a unit circle centered around particle i, including itself). The influence of the neighbors is through an average angle

$$\langle \theta_i(t) \rangle_r = \Theta \left[\sum_{j:\, d_{ij}<1} \boldsymbol{v}_j(t) \right], \tag{15}$$

where $\Theta[\boldsymbol{v}]$ represents the angle of vector $\boldsymbol{v}$ and d_{ij} is the distance between particles i and j. The evolution is

$$\boldsymbol{x}_i(t+\Delta t) = \boldsymbol{x}_i(t) + \boldsymbol{v}_i(t+\Delta t)\Delta t, \tag{16}$$

$$\theta_i(t+\Delta t) = \langle \theta_i(t) \rangle_r + \eta \xi_i(t). \tag{17}$$

Here the key ingredient is the competition between the tendency towards local alignment and the angular noise $\xi_i(t)$ that might come from external perturbations and/or from uncertainties in individual's perception, chosen from a uniform distribution within the interval $[-1/2, 1/2]$. The amplitude of noise η has a maximum value $\eta_{\max} = 2\pi$. In the absence of noise with $\eta = 0$, all particles tend to align perfectly.

For SVM, $\bar{v} = v_0$, $\bar{v}_{i,x} = \cos\theta_i$, and $\bar{v}_{i,y} = \sin\theta_i$. Our simulations are started with all particles distributed randomly in the domain. To overcome the dependence on the initial conditions, the first 2×10^5 microstates are neglected. The subsequent microstates are chosen at an interval of 40 steps to keep independence. We take $M = 2 \times 10^4$ microstates to get an ensemble matrix $\boldsymbol{A}$. Its eigenvalues and eigen microstates can be calculated afterwards.

The probabilities of the eigen microstates are presented in Fig. 1. Under strong noises, no eigen microstate is dominant and the system is in disorder. With the decrease of η, σ_1 becomes finite and a phase $\boldsymbol{u}_1$ emerges at first. Further, two degenerate eigen microstates $\boldsymbol{u}_2$ and $\boldsymbol{u}_3$ appear simultaneously.

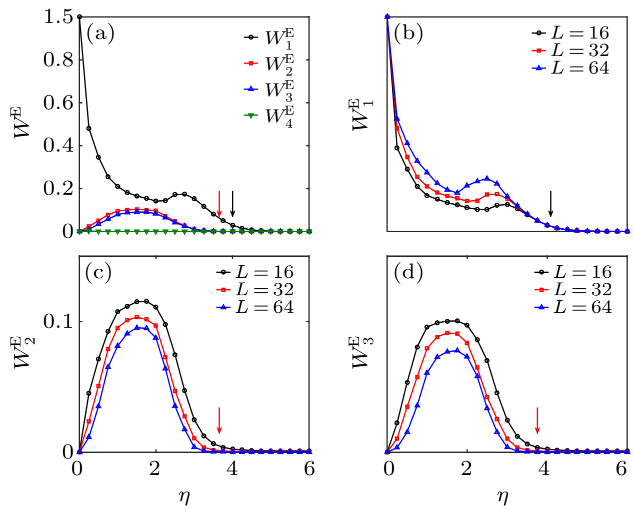

Fig. 1. Probabilities $W_I^{\rm E}$ of eigen microstates in SVM with $\rho = 2, v_0 = 0.5$. (a) Different probabilities at $L = 32$. (b) $W_1^{\rm E}$ at different sizes. (c) $W_2^{\rm E}$ at different sizes. (d) $W_3^{\rm E}$ at different sizes. The phase transition point of $\boldsymbol{u}_1$ is indicated by the black arrow and that of $\boldsymbol{u}_{2,3}$ by the red arrow.

To identify the phase transition point and type of phase transition, we investigate the size dependence of $W_I^{\rm E}(\eta, L)$. According to Eq. (12), we have

$$\ln W_I^{\rm E}(\eta, L) = -2\beta/\nu \ln L + 2\ln f_I(hL^{1/\nu}). \tag{18}$$

There is a linear dependence of $\ln W_I^{\rm E}$ on $\ln L$ at $h = 0$. This can be used to determine the transition point and critical exponent ratio β/ν at the same time.

It has been manifested in Fig. 2(a) that $W_1^{\rm E}$ has a jump at $\eta_{1c} = 3.95$, which indicates a discontinuous phase transition of $\boldsymbol{u}_1$. In Figs. 2(b) and 2(c), a continuous phase transition of $\boldsymbol{u}_2$ and $\boldsymbol{u}_3$ at $\eta_{2c} = 3.69$ is identified. It has the ratio of critical exponent $\beta/\nu = 0.94$.

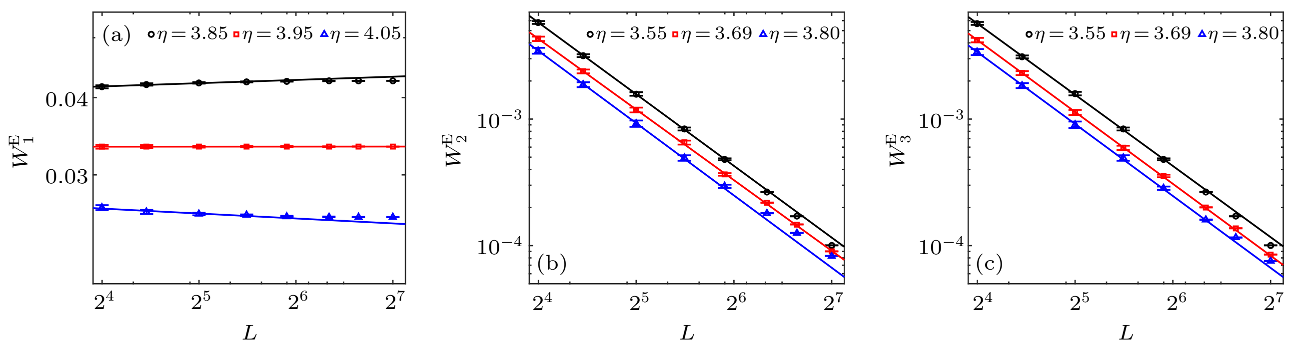

Fig. 2. Log–log plot of $W_I^{\rm E}$ versus L around transition points. (a) $W_1^{\rm E}$ with $\eta_{1c} = 3.95$ and $\beta_1/\nu_1 = -0.0000(5)$. (b) $W_2^{\rm E}$ with $\eta_{2c} = 3.69$ and $\beta_2/\nu_2 = 0.94(1)$. (c) $W_3^{\rm E}$ with $\eta_{3c} = 3.69$ and $\beta_3/\nu_3 = 0.94(2)$.

To characterize the physical character of the phase transitions above, we calculate the collective motion index and density fluctuation index of eigen microstate and present them in Fig. 3. In the eigen microstates, velocity and density are correlated. This is similar to the magnetic lattice gas,[28] where the orientation and density of the particle are correlated.

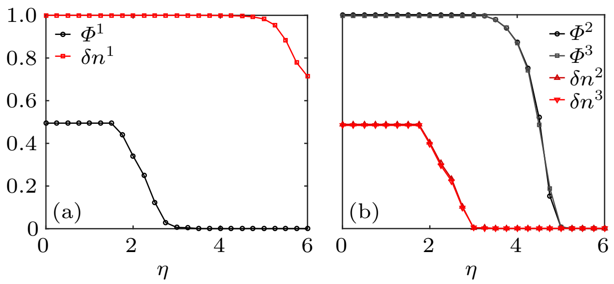

Fig. 3. Collective motion index Φ^I and density fluctuation index δn^I of SVM with size $L = 64$. (a) $I = 1$. (b) $I = 2, 3$.

At η_{1c}, $\boldsymbol{u}_1$ has zero collective motion index Φ and nonzero density fluctuation index δn. Therefore, $\boldsymbol{u}_1$ has a discontinuous transition of density. At η_{2c}, both $\boldsymbol{u}_2$ and $\boldsymbol{u}_3$ have nonzero Φ and zero δn. Here there is a continuous transition of velocity.

The spatial distributions of eigen microstates are shown in Figs. 4 and 5 for $\boldsymbol{u}_1$ and $\boldsymbol{u}_2$, respectively. In Fig. 6, the velocities and density fluctuations of eigen microstates $\boldsymbol{u}_3$ are shown for different noises. The velocity direction of $\boldsymbol{u}_3$ is orthogonal to that of $\boldsymbol{u}_2$.

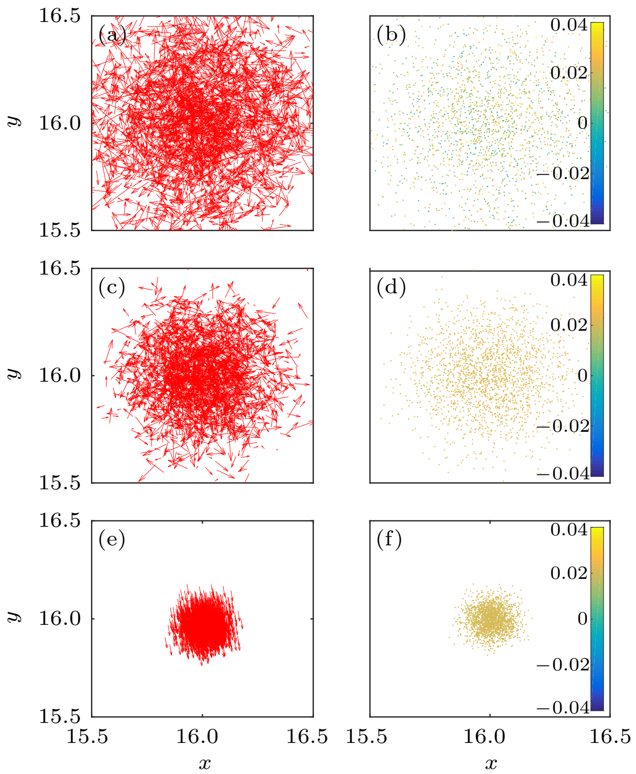

Fig. 4. Spatial distributions of velocity (a), (c), (e) and neighborhood density fluctuation (b), (d), (f) for $\boldsymbol{u}_1$ under noises $\eta = 6, \eta_{1c} = 3.95$, and 0.25 respectively.

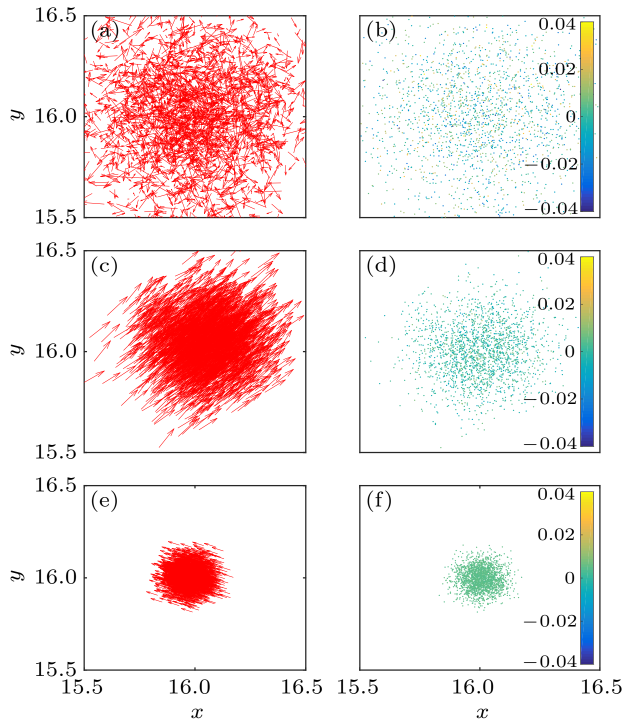

Fig. 5. Spatial distribution of velocity (a), (c), (e) and neighborhood density fluctuation (b), (d), (f) for $\boldsymbol{u}_2$ under noises $\eta = 6, \eta_{2c} = 3.69$, and 0.25 respectively.

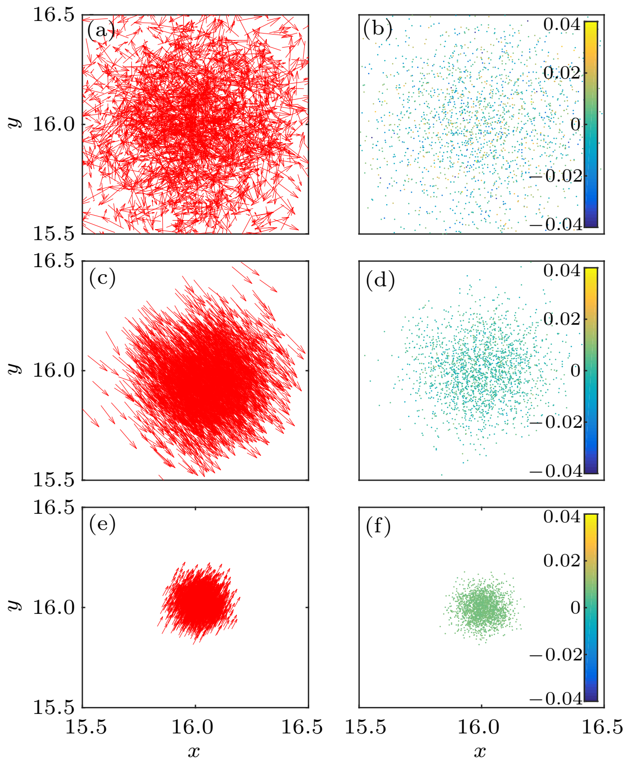

Fig. 6. Spatial distribution of velocity (a), (b), (c) and neighborhood density fluctuation (d), (e), (f) for $\boldsymbol{u}_3$ of SVM under noises $\eta = 6$, $\eta_{3c} = 3.69$ and 0.25. The velocity direction of $\boldsymbol{u}_3$ is orthogonal to that of $\boldsymbol{u}_2$.

To understand the peak of W_1^{E} in Fig. 1, we study the noise dependence of $\bar{n}$ in Fig. 7. With the decrease of noise, $\bar{n}$ increases at first. This is in accord with the condensation of $\boldsymbol{u}_1$. Afterwards there is a decrease of $\bar{n}$. The peak becomes more prominent with the increase of L. These phenomena were found also in Ref. [29].

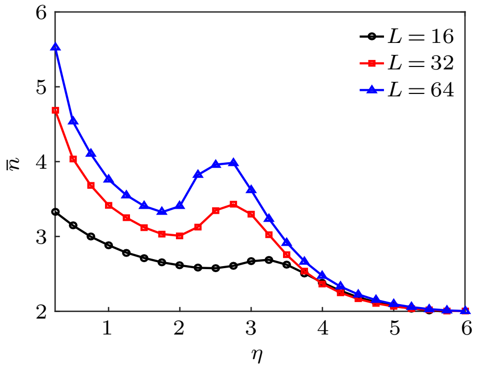

Fig. 7. Average particle density $\bar{n}$ as a function of noise.

To investigate the density dependence of the phase transitions, we study also the SVM at densities $\rho = 1, 3$ in addition. There are also discontinuous phase transitions of density at first and then continuous phase transitions of velocity in these systems. With the increase of density, the discontinuous transition of density appears at larger noise. We have obtained $\eta_{1c} = 3.18$ at $\rho = 1$, $\eta_{1c} = 3.95$ at $\rho = 2$, and $\eta_{1c} = 4.3$ at $\rho = 3$. As shown in Figs. 2, 9, and 10, the jump of order-parameter decreases with increasing density.

Correspondingly, the continuous transition points $\eta_{2c,3c}$ increase with increasing density. We get $\eta_{2c,3c} = 3.06$ at $\rho = 1$, $\eta_{2c,3c} = 3.65$ at $\rho = 2$, and $\eta_{2c,3c} = 4.0$ at $\rho = 3$. The same ratio of critical exponent β/ν has been obtained for the different continuous phase transitions, which belong to the same universality class.

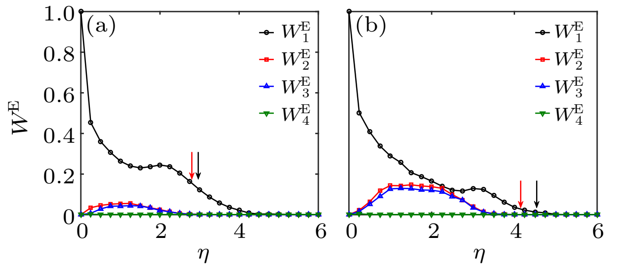

Fig. 8. Probabilities of the first four eigen microstates for SVM with $L = 32$ and densities (a) $\rho = 1$, (b) $\rho = 3$ (b). The phase transition point of $\boldsymbol{u}_1$ is indicated by the black arrow and that of $\boldsymbol{u}_{2,3}$ by the red arrow.

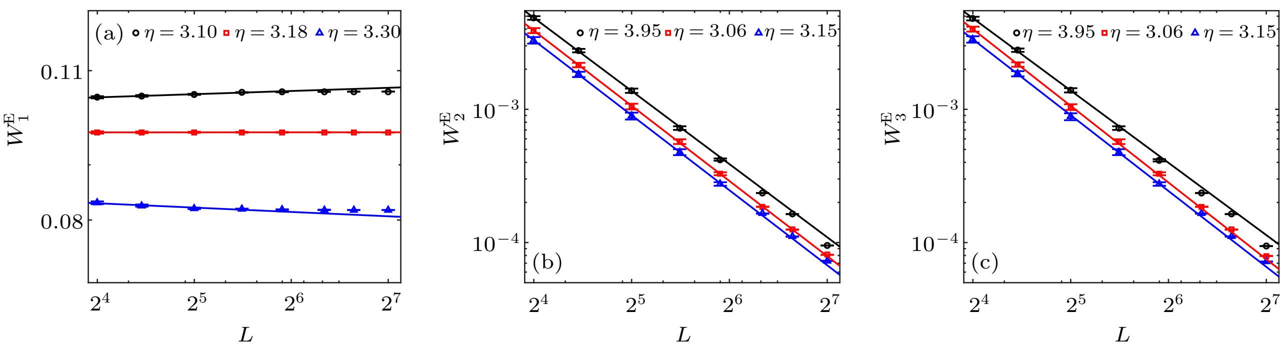

Fig. 9. Log–log plot of $W_I^{\rm E}$ versus L for SVM with $\rho = 1$. (a) $W_1^{\rm E}$ with $\eta_{1c} = 3.18$ and $\beta_1/\nu_1 = -0.0001(7)$. (b) $W_2^{\rm E}$ with $\eta_{2c} = 3.06$ and $\beta_2/\nu_2 = 0.94(3)$. (c) $W_3^{\rm E}$ with $\eta_{3c} = 3.06$ and $\beta_3/\nu_3 = 0.93(9)$.

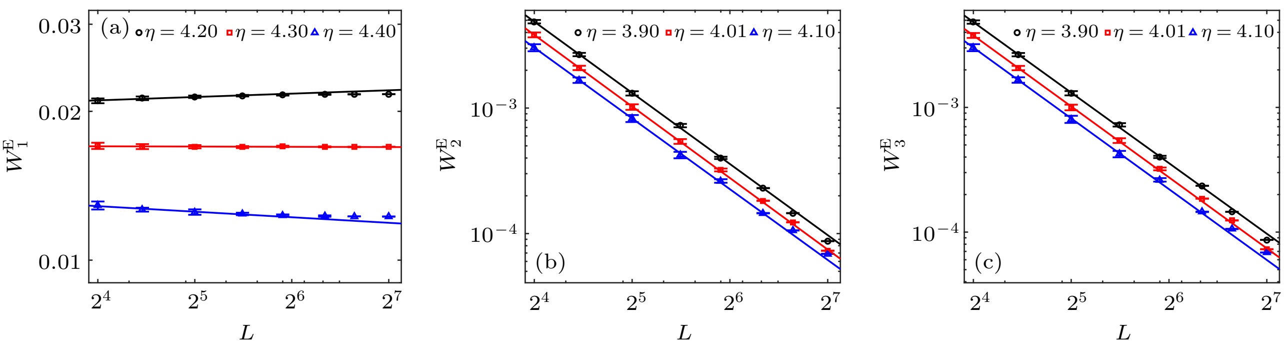

Fig. 10. Log–log plot of $W_I^{\rm E}$ versus L for SVM with $\rho = 3$. (a) $W_1^{\rm E}$ with $\eta_{1c} = 4.3$ and $\beta_1/\nu_1 = 0.0001(7)$. (b) $W_2^{\rm E}$ with $\eta_{2c} = 4.01$ and $\beta_2/\nu_2 = 0.94(3)$. (c) $W_3^{\rm E}$ with $\eta_{3c} = 4.01$ and $\beta_3/\nu_3 = 0.94(1)$.

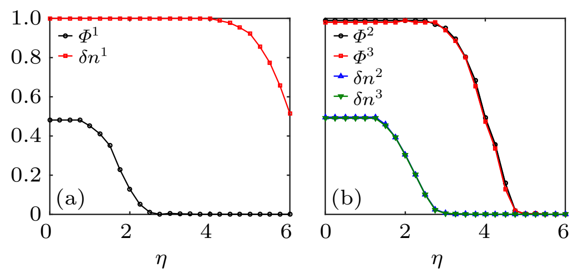

Fig. 11. Collective motion Φ^I and density fluctuation δn^I of SVM with $L = 32$ and $\rho = 1$.

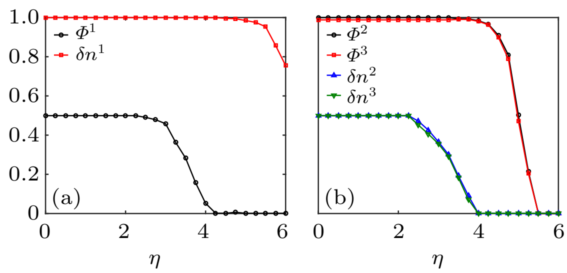

Fig. 12. Collective motion Φ^I and density fluctuation δn^I of SVM with $L = 32$ and $\rho = 3$.

To explore the generality of the phase transitions found in SVM, we study the hierarchical Vicsek model (HVM),[30] which is a generalized version of SVM.

3.2. HVM

In the HVM, all particles are ordered by their hierarchical rank j with $j=1$ being the highest and $j=N$ the lowest. For particle i, the influence of a lower-ranked particle $j \leq i$ is reduced by a factor $\alpha < 1$. Instead of Eq. (10), the average angle here is

$$\langle \theta_i(t) \rangle_r = \Theta\left[\sum_{d_{ij}<1,\, j\leq i} \boldsymbol{v}_j(t) + \alpha \sum_{d_{ij}<1,\, j>i} \boldsymbol{v}_j(t) \right]. \quad (19)$$

SVM is recovered by $\alpha = 1$.

We have studied the HVMs at $\alpha = 1/9, 1/36$. In Fig. 13, the probabilities of the first four eigen microstates are presented for $\alpha = 1/9$ in (a) and $\alpha = 1/36$ in (b). Their transition points are determined in Figs. 14 and 15 and indicated by arrows. With the decrease of α, the peaks of W_1^{E} and $W_{2,3}^{\mathrm{E}}$ increase.

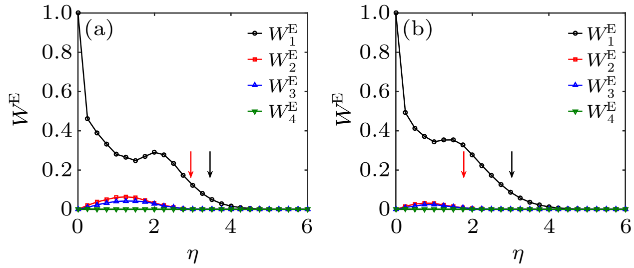

Fig. 13. Probabilities of HVM with $L=32$, $\rho=2$ and hierarchical factors: (a) $\alpha=1/9$, (b) $\alpha=1/36$. The transition points are indicated by arrows.

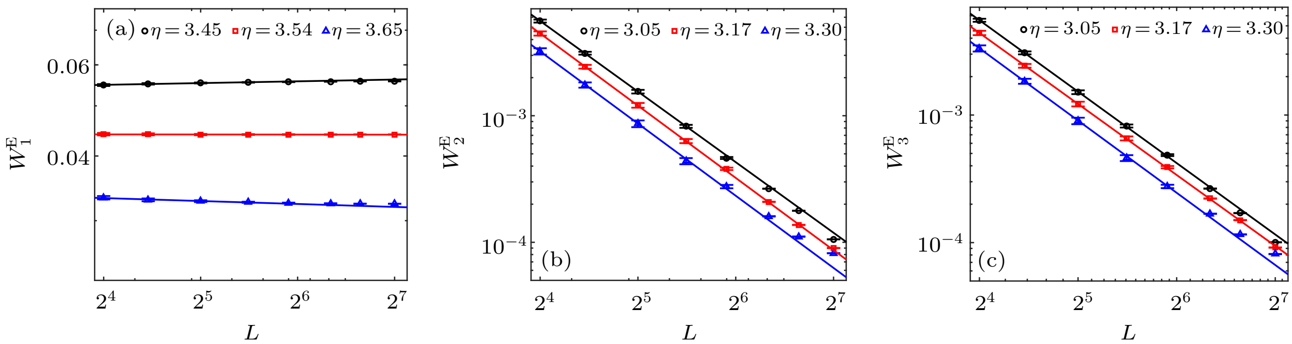

Fig. 14. Log–log plot of W_I^{E} versus L for the HVM with $\alpha=1/9$. (a) W_1^{E} with $\eta_{1\mathrm{c}}=3.54$ and $\beta_1/\nu_1=-0.0000(1)$. (b) W_2^{E} with $\eta_{2\mathrm{c}}=3.17$ and $\beta_2/\nu_2=0.94(4)$. (c) W_3^{E} with $\eta_{3\mathrm{c}}=3.17$ and $\beta_3/\nu_3=0.93(8)$.

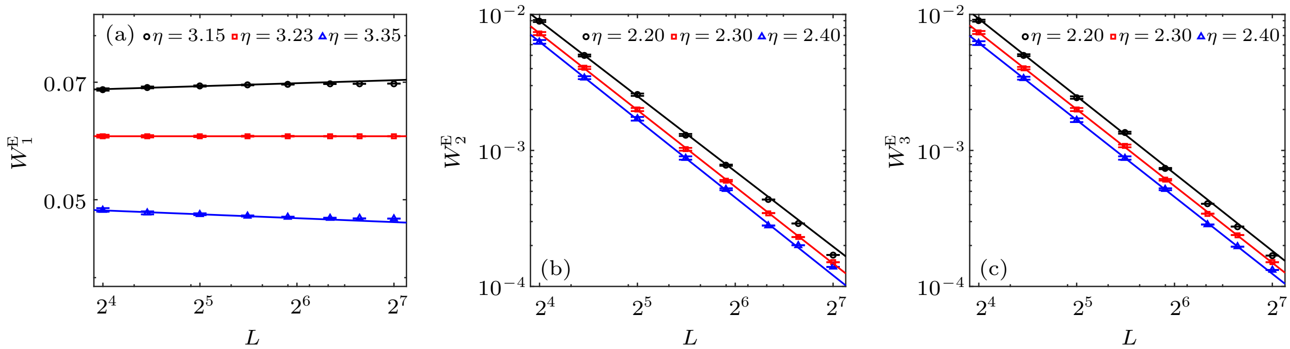

Fig. 15. Log–log plot of W_I^{E} versus L for the HVM with $\alpha=1/36$. (a) W_1^{E} with $\eta_{1\mathrm{c}}=3.23$ and $\beta_1/\nu_1=-0.0000(3)$. (b) W_2^{E} with $\eta_{2\mathrm{c}}=2.3$ and $\beta_2/\nu_2=0.94(2)$. (c) W_3^{E} with $\eta_{3\mathrm{c}}=2.3$ and $\beta_3/\nu_3=0.94(1)$.

Because of the hierarchical rank in HVM, the discontinuous phase transition of $\boldsymbol{u}_1$ is delayed by the hierarchical factor α so that $\eta_{1\mathrm{c}}=3.95$ for $\alpha=1$, $\eta_{1\mathrm{c}}=3.54$ for $\alpha=1/9$, and $\eta_{1\mathrm{c}}=3.23$ for $\alpha=1/36$. Correspondingly, the jump at the discontinuous transition of density increases as $W_1^{\mathrm{E}}(\eta_{1\mathrm{c}},L)=0.035$ at $\alpha=1$, $W_1^{\mathrm{E}}(\eta_{1\mathrm{c}},L)=0.043$ at $\alpha=1/9$, and $W_1^{\mathrm{E}}(\eta_{1\mathrm{c}},L)=0.060$ at $\alpha=1/36$.

The continuous phase transitions of HVM are also delayed so that $\eta_{2\mathrm{c},3\mathrm{c}}=3.65$ at $\alpha=1$, $\eta_{2\mathrm{c},3\mathrm{c}}=3.17$ at $\alpha=1/9$, and $\eta_{2\mathrm{c},3\mathrm{c}}=2.3$ at $\alpha=1/36$. The ratios β/ν at different α are the same. So the continuous phase transitions of SVM and HVM belong to the same universality class. We summarize the results obtained above in Table 1.

Table 1. Summary of transition points and ratios of critical exponents.

	$\eta_{1\mathrm{c}}$	β_1/ν_1	$\eta_{2\mathrm{c}}$	β_2/ν_2	β_3/ν_3
SVM					
$\rho=1$	3.18	−0.0001(7)	3.06	0.94(3)	0.93(9)
$\rho=2$	3.95	0.0000(5)	3.65	0.94(1)	0.94(2)
$\rho=3$	4.30	0.0001(7)	4.01	0.94(3)	0.94(1)
HVM ($\rho=2$)					
$\alpha=1/9$	3.54	−0.0000(1)	3.17	0.94(4)	0.93(8)
$\alpha=1/36$	3.23	−0.0000(3)	2.30	0.94(2)	0.94(1)

Our studies above show that particles in the living systems with strong noise have random positions and velocities. With the decrease of noise, the interactions between the particles make them get closer and the average density $\bar{n}$ becomes larger, as shown in Fig. 7. These interactions result in a gas-liquid like transition of density, which is discontinuous. With further decrease of noise, particles stay further closer to each other and the average density $\bar{n}$ becomes larger. The even stronger interactions between particles make the directions of velocity become ordered and there is a phase transition of collective motion, which is continuous.

4. Conclusions

We propose a method for investigating phase emergence and transitions in living systems under the framework of eigen microstate. From the velocity and position sequences of particles in a living system, we define a normalized ensemble matrix $\boldsymbol{A}$ with columns and rows corresponding to microstates and time sequences of the particles. $\boldsymbol{A}$ can be decomposed as the sum of eigen microstate $\boldsymbol{u}_I$ multiplied by its time sequence $\boldsymbol{v}_I$ and eigen value σ_I, where $\sum_I \sigma_I^2 = 1$. A finite σ_I in the thermodynamic limit reveals the emergence of $\boldsymbol{u}_I$. Near transition point $h = 0$, σ_I follows a finite-size scaling form $\sigma_I(h,L) = L^{-\beta/\nu} f_I(hL^{1/\nu})$, with $\beta > 0$ and $\beta = 0$ for continuous and discontinuous phase transitions, respectively.

The phase emergence and transitions of both SVM[19] and HVM[30] have been investigated. With the decrease of noise, we find at first phase emergence of density with $\beta = 0$. So the corresponding phase transitions are discontinuous. At even smaller noises, there is the phase emergence of velocity with $\beta/\nu = 0.94$ and the phase transitions are continuous and belong to the same universality class.

Our results demonstrate that the eigen microstate approach works for nonequilibrium systems. Our approach can be applied not only to living systems but also to other complex systems, such as climate systems,[23,31] ecosystems,[32] *et al.*

Acknowledgment

We thank Profs. Li Chen and Xiaqing Shi for helpful discussions.

References

[1] Cavagna A, Cimarelli A, Giardina I, Parisi G, Santagati R, Stefanini F and Viale M 2010 *Proc. Natl. Acad. Sci. USA* **107** 11865
[2] Bialek W, Cavagna A, Giardina I, Mora T, Silvestri E, Viale M and Walczak A M 2012 *Proc. Natl. Acad. Sci. USA* **109** 4786
[3] Bialek W, Cavagna A, Giardina I, Mora T, Pohl O, Silvestri E, Viale M and Walczak A M 2014 *Proc. Natl. Acad. Sci. USA* **111** 7212
[4] Chen X, Dong X, Be'er A, Swinney H L and Zhang H 2012 *Phys. Rev. Lett.* **108** 148101
[5] Li H, Shi X q, Huang M, Chen X, Xiao M, Liu C, Chaté H and Zhang H 2019 *Proc. Natl. Acad. Sci. USA* **116** 777
[6] Feinerman O, Pinkoviezky I, Gelblum A, Fonio E and Gov N S 2018 *Nat. Phys.* **14** 683
[7] Altshuler E, Ramos O, Núñez Y, Fernández J, Batista-Leyva A and Noda C 2005 *The American Naturalist* **166** 643
[8] Buhl J, Sumpter D J, Couzin I D, Hale J J, Despland E, Miller E R and Simpson S J 2006 *Science* **312** 1402
[9] Attanasi A, Cavagna A, Del Castello L, *et al.* 2014 *Phys. Rev. Lett.* **113** 238102
[10] Attanasi A, Cavagna A, Del Castello L, *et al.* 2014 *PLoS Computational Biology* **10** e1003697
[11] Ginelli F, Peruani F, Pillot M H, Chaté H, Theraulaz G and Bon R 2015 *Proc. Natl. Acad. Sci. USA* **112** 12729
[12] Krause J, Ruxton G D, Ruxton G, *et al.* 2002 *Living in Groups* (Oxford University Press)
[13] Sumpter D J 2010 *Collective Animal Behavior* (Princeton University Press)
[14] Marchetti M C, Joanny J F, Ramaswamy S, Liverpool T B, Prost J, Rao M and Simha R A 2013 *Rev. Mod. Phys.* **85** 1143
[15] Sethna J 2021 *Statistical mechanics: entropy, order parameters, and complexity*, volume 14 (Oxford University Press, USA)
[16] Anderson P W 1972 *Science* **177** 393
[17] Wilson K G 1979 *Scientific American* **241** 158
[18] Barmatz M, Hahn I, Lipa J and Duncan R 2007 *Rev. Mod. Phys.* **79** 1
[19] Vicsek T, Czirók A, Ben-Jacob E, Cohen I and Shochet O 1995 *Phys. Rev. Lett.* **75** 1226
[20] Grégoire G and Chaté H 2004 *Phys. Rev. Lett.* **92** 025702
[21] Chaté H, Ginelli F, Grégoire G and Raynaud F 2008 *Phys. Rev. E* **77** 046113
[22] Hu G, Liu T, Liu M, Chen W and Chen X 2019 *Science China Physics, Mechanics & Astronomy* **62** 990511
[23] Sun Y, Hu G, Zhang Y, Lu B, Lu Z, Fan J, Li X, Deng Q and Chen X 2021 *Commun. Theor. Phys.* **73** 065603
[24] Gibbs J W 1902 *Elementary principles in statistical mechanics developed with especial reference to the rational foundation of thermodynamics* (New York: C. Scribner)
[25] Griffin A, Snoke D W, and Stringari S 1996 *Bose–Einstein Condensation* (Cambridge University Press)
[26] Li X T and Chen X S 2016 *Commun. Theor. Phys.* **66** 355
[27] Strang G, Strang G, Strang G and Strang G 1993 *Introduction to Linear Algebra* volume 3, (Wellesley: Wellesley-Cambridge Press)
[28] Li L, Chen W, Dong W and Chen X 2011 *Euro. Phys. J. B* **80** 189
[29] Huepe C and Aldana M 2008 *Physica A* **387** 2809
[30] Xue T, Li X, Grassberger P and Chen L 2020 *Phys. Rev. Research* **2** 042017
[31] Lenton T M, Held H, Kriegler E, Hall J W, Lucht W, Rahmstorf S and Schellnhuber H J 2008 *Proc. Natl. Acad. Sci. USA* **105** 1786
[32] Scheffer M, Carpenter S R, Lenton T M, *et al.* 2012 *Science* **338** 344